

12-2015

Response of Bacterial Cells to Fluctuating Environment

Sudip Nepal

University of Arkansas, Fayetteville

Follow this and additional works at: <http://scholarworks.uark.edu/etd>



Part of the [Biophysics Commons](#), and the [Cell Biology Commons](#)

Recommended Citation

Nepal, Sudip, "Response of Bacterial Cells to Fluctuating Environment" (2015). *Theses and Dissertations*. 1404.
<http://scholarworks.uark.edu/etd/1404>

This Thesis is brought to you for free and open access by ScholarWorks@UARK. It has been accepted for inclusion in Theses and Dissertations by an authorized administrator of ScholarWorks@UARK. For more information, please contact scholar@uark.edu.

Response of Bacterial Cells to Fluctuating Environment

A thesis submitted in partial fulfillment
of the requirements for the degree of
Master of Science in Physics

by

Sudip Nepal
Tribhuvan University
Master of Science, 2008
Tribhuvan University
Bachelor of Science in Physics, 2005

December 2015
University of Arkansas

This thesis is approved for recommendation to the Graduate Council.

Dr. Pradeep Kumar
Thesis Advisor

Dr. Ravi Damodar Barabote
Committee Member

Dr. Woodrow L. Shew
Committee Member

Dr. Jiali Li
Committee Member

Dr. Reeta Vyas
Committee Member

Abstract

We have studied morphological and genomic variations occurring in a mesophilic bacterium *Escherichia coli* (*E. coli*) in a wide range of continuous and fluctuating hydrostatic pressures. For all the studies here the temperature is maintained at 37°C, the optimal growth temperature of *E. coli* at atmospheric pressure. Cell division is inhibited at high hydrostatic pressures resulting in an increase of cell length. The increase of cell-length depends on the extent and duration of the stress applied on bacterial cells. We have studied the effect of high pressure stress in three different conditions – (i) Wild-type cells (almost no genetic mutations), (ii) cells cloned with a plasmid DNA containing *mreB* gene under *lac* promoter (but no induction of the gene expression), and (iii) cells cloned with a plasmid DNA containing *mreB* gene with induction of the gene expression. We find that, the cellular response of the cells is different in the three cases studied here. Specifically, we find that, the wild-type bacteria with no addition of a plasmid DNA are stressed the least at high pressure as compared to bacterial cells containing plasmid DNA. Moreover, our results suggest that, the cells containing a plasmid DNA upon induction of the gene expression are stressed the most and exhibit higher propensity of lack of cell division at high pressure. We have quantified the propensity of lack of cell division in different conditions by quantifying the probability distribution of the cell length. We find that, the probability distribution of the length of bacterial cells with a plasmid DNA show multiple peaks whereas wild-type bacterial cells show single peaked distribution. Next, we applied the oscillatory pressure. We find that, the average cell-length of bacteria decreases with τ suggesting that, the elongation of cells at high pressure is reversible. It is observed that the average length ($\langle \ell \rangle$) of the bacterial cells revert back to the length of the bacterial cells at atmospheric pressure for $\tau \approx 20$ minutes for all the cases studied here.

Dedication

This thesis is dedicated to my parents who showed me path in every step of my life and always encouraged me to do research work. They are the greatest source of inspiration for me to carry out my coursework as well as research work.

Acknowledgement

I would like to show extreme gratitude to my thesis advisor, Dr. Pradeep Kumar. His advising and mentoring helped me to complete the project as well as my thesis in a very short period of time. This work would have been impossible without his proper guidance. I admire his continuous dedication towards research and students' progress which always motivated me to complete this project with great passion.

I am thankful to my thesis committee members: Dr. Jiali Li (Physics Department), Dr. Reeta Vyas (Physics Department), Dr. Woodrow L. Shew (Physics Department) and Dr. Damodar Ravi Barabote (Biology Department), for their great support, guidance and suggestion during this project.

Finally, I would like to thank my friends Mr. Prashant Acharya, Desalegn Tadesse Debu, Samir Jha, and Bhuwan Khatri for their moral support, advice, and inspiration.

Table of Contents

• Title of Thesis	
• Abstract	
• Acknowledgements	
• Contents	
• List of Figures	
• List of Symbols	
• Introduction	1
• Escherichia coli (E. coli) as a model organism	2
• Plasmid DNA	5
• Motivation	6
• Research objective	7
• Thesis outline	7
• Experimental setup and microbiology protocols	8
• Bacterial Strain	8
• Cell culture and media	8
• High pressure setup	8
• Imaging and analysis of the images	9
• Phenotypic changes of bacterial cells under continuous and oscillatory pressure	10
• Response of wild-type cells (E. coli strain MC4100)	10
• Comparison of morphology at normal and high continuous pressures	10
• Comparison of morphology at different relaxation time(τ)	12
• Response of wild-type MC4100 to fast oscillations in pressure	16
• Morphology at different relaxation time after growing to saturation regime(τ)	16
• Response of MC4100 cloned with a plasmid DNA	19
• Comparison of morphology of at normal and at high continuous pressures	19

• Comparison of morphology at different relaxation time(τ)	22
• Comparison of $\langle \ell \rangle$ different τ for different strains of bacterial cells	24
• Comparison of morphology of wild-type MC4100 and MC4100 cloned with a plasmid DNA at continuous high pressure	26
• Theoretical model to explain cell-length variability	28
• Stochastic cell division of two populations	28
• Theoretical model with two sub-populations	29
• Discussion	32
• Conclusion	33
• Bibliography	35
• Appendix	38

List of Figures

Fig.1 Schematic of cell division of <i>Escherichia coli</i>	2
Fig.2 Growth curve of bacteria	3
Fig.3 Schematic of a plasmid DNA	6
Fig.4 Experimental setup for high pressure system	9
Fig.5 Morphology and probability distribution of cell length of wild-type MC4100 at continuous pressures	11
Fig.6 Probability distributions of cell length of wild-type MC4100 at different relaxation times	14
Fig.7 Relaxation time dependence of average length at oscillatory pressure	15
Fig.8 Comparison of morphology of cell length of wild-type MC4100 at different oscillatory pressures applied after growing to saturation regime	17
Fig.9 Relaxation time dependence of average length at oscillatory pressure after growing to saturation regime	18
Fig.10 Representative images and probability distribution of MC4100 cloned with a plasmid DNA	20
Fig.11 Relaxation time dependence of average length of MC4100 cloned with a plasmid DNA at oscillatory pressure	22
Fig.12 Relaxation time dependence of average length of MC4100 cloned with a plasmid DNA at oscillatory pressure	23
Fig.13 Relaxation time dependence of average length of different samples at oscillatory pressure	25
Fig.14 Probability distribution of cell length of wild-type MC4100 and MC4100 cloned with a plasmid DNA at continuous pressure of 400 latm	26
Fig.15 Schematic of cell division of two populations	29
Fig.16 Theoretical model fit to the experimental data	31

List of Symbols

τ = Relaxation time

ℓ = Length of bacterial cell

$\langle \ell \rangle$ = Average cell length

$P(\ell)$ = Probability distribution

T = Population doubling time for bacteria

P = Pressure

ℓ_0 = Average length corresponding to 1 atm pressure and 37° C

σ_0 = Standard deviation of distribution of the cell length of the bacteria at atmospheric pressure and 37° C

β = Pressure-temperature dependent probability of lack of cell division

$\beta = 1 - \alpha$ = Pressure-temperature dependent probability of cells to divide normally

n = Number of generations

List of Abbreviations

E. coli : *Escherichia coli*

atm: Atmospheric pressure

μm : Micro meter

DNA: Deoxyribonucleic Acid

IPTG: Isopropyl β -D-1-Thiogalactopyranoside

GTP: Guanosine 5-Tri-Phosphate

ATP: Adenosine Tri-Phosphate

ADP: Adenosine Di-Phosphate

GFP: Green Fluorescent Protein

LB: Luria Broth

OD: Optical Density

Introduction

Living organisms can live and thrive in different environmental conditions. Prokaryotes like archaea and bacteria can live and grow in diverse environmental conditions. For example, a large number of bacteria and archaea can thrive at high hydrostatic pressure, under the deep sea surface [1, 2], under the subsurface of rocks [3]. Those bacteria that can only grow at high pressures are called obligatory barophiles [4]. Bacteria can also live and thrive in a wide range of temperature. Bacteria that grow at moderate temperature are called mesophiles ($30 - 47^{\circ}\text{C}$). Thermophiles grow at high temperatures ($50 - 60^{\circ}\text{C}$). Bacteria that grow at low temperatures ($15 - 20^{\circ}\text{C}$) are termed as psychrophiles. Beside temperature and pressure, there are different environmental conditions in which bacteria can grow and survive. Acidophiles, alkaliphiles, xerophiles, radiotolerant are examples of bacteria and archaea that grow in low pH, high pH, low water, high radiation respectively [5, 6, 7, 8, 9].

Organisms typically exhibit an optimality of cellular processes and life activities at specific environmental conditions. For example, *Escherichia coli* (*E. coli*), a mesophilic bacterium, exhibits optimal cellular activities at 37°C temperature and atmospheric pressure, resulting into the maximum growth rate [10] at these conditions. Organisms encounter environmental fluctuations including the fluctuations in nutrients, temperature, pressure, pH, salt concentrations, radiation. The environmental fluctuations may give rise to deviation in characteristics of an organism. The deviation in characteristics of an organism can broadly be classified under two categories namely genotypic and phenotypic. Those species that can adapt themselves in a given environmental fluctuations survive whereas others vanish from the nature. Pressure and temperature can change the time scales of cellular process since both pressure and temperature affect the not only the stability and hence the functionality of biomolecules but can also change the rate of different chemical processes inside the cell. One important question that arises is if the cells are exposed to non-optimal conditions (stresses) what time-scales over which they come back to normal state when those stresses are removed. In order to probe the time-scale of reversibility of bacterial cells upon applica-

tion and removal of non-optimal environmental conditions, we have investigated the cellular response of a mesophilic bacterium to fluctuations in hydrostatic pressure.

Below, we describe the model bacteria used for these studies. We also briefly summarize the earlier results of the response of the cells to high pressure and extremes of temperature.

Escherichia coli (E. coli) as a model organism

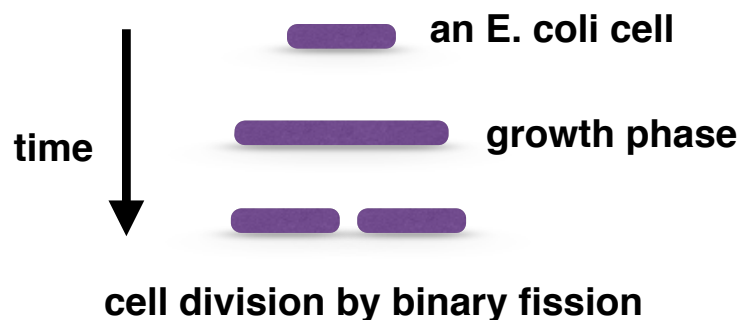


Figure 1: Schematic of cell division of *Escherichia coli*.

E. coli is the most studied bacteria and hence serves as a good prokaryotic model organism. Fast population doubling and growth in a wide range of temperatures and pressures have made *E. coli* an ideal candidate for studying prokaryotic cellular processes in laboratory settings. *E. coli* reproduces asexually, by the method of binary fission. A mother cell grows in length about twice its original length. Then the mother cell divides into two identical daughter cells. A schematic of the cell division process is shown in Fig. 1.

Growth rate of bacterial cells is concentration dependent. The concentration of bacteria in a media can be determined using optical density (OD). So the curve obtained by plotting OD versus time is a growth curve. Growth curve of bacteria has three distinct regions: an early phase where growth is very small called lag phase, an intermediate phase where cellular activities are maximum resulting in a maximum growth rate is known as exponential phase, a late phase at which the growth rate of bacteria almost stops and even may start to die due

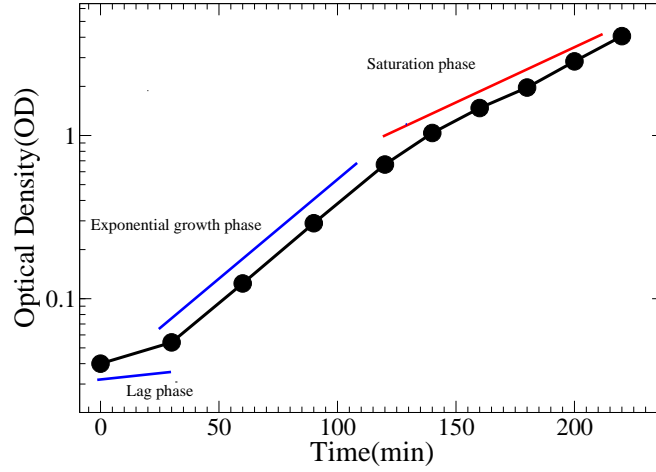


Figure 2: A typical growth curve of bacterial cell. Optical density of the sample is shown as a function of time on a linear-log plot. The data were obtained at $P=1\text{atm}$ and $T=37^\circ$

to starvation termed as saturation phase [11]. The growth rate of bacteria tells us the rate of increase of bacterial biomass.

During the growth part of the cell division, the genomic DNA within the cell is replicated which are acquired by the two daughter cells at the end of the division process. Other macromolecules such as RNA, proteins, and other regulatory molecules available in the mother cell are distributed more or less evenly between two daughter cells [12]. Cell division process is an interesting process as a cell undergoes many changes during this phase. When a cell is ready to divide it forms a partition, the site for cell division. Recent studies suggest that the partition may not occur exactly at the mid point of the cell. The process of partitioning is a stochastic process [13, 14, 15, 15, 16, 17, 18, 19, 20]. So far nine different genes (*ftsA*, *ftsI*, *ftsL*, *ftsN*, *ftsO*, *ftsW*, *ftsZ* and *zipA*) localize at the site of the division in *E. coli* [21, 22, 23, 24, 25, 26, 27, 28] and regulate the cell division in one way or another. The role of all these genes in cell division still unclear. Among these, *ftsZ* plays a very important role in the cell division. division [29]. The aggregation of the proteins and capability of *ftsZ*

to GTPase activity and hydrolysis of GTP causes the formation of Z-ring [30]. *ftsZ* protein itself can apply the contractile force to the ring to such that constriction occurs in the cell resulting into division [31]. Under high pressures *ftsZ* protein polymerizes to form filament resulting no formation of the Z-ring. So at high pressures there is inhibition of the cell division [32]. The formation of Z-ring decreases on increasing hydrostatic pressure results in higher inhibition of cell division at high hydrostatic pressures [13].

E. coli exhibits maximum cellular activity and growth rate at atmospheric pressure and 37° C. When the environmental condition deviates from the optimal growth conditions, the cellular activity of *E. coli* decreases resulting in a decrease of growth rate of the cells. For example growth rate of *E. coli* decreases upon increasing or decreasing the temperature from 37°C. The effect of temperature on growth and morphology of *E. coli* is well known. Effect of pressure is relatively less explored. Cellular activities of the bacteria decrease at high hydrostatic pressures resulting in smaller growth rate [33, 34]. This indicates that the survival rate of the bacteria becomes lower upon increasing the pressure. Cellular activities of the cells depend on magnitude and time of the stress (non-optimal or unfavorable environmental conditions) applied. *E. coli* cells can grow and divide when pressure is less than 250 atm [33]. The growth rate inhibits and elongation of cells occurs at the pressure of 300 – 500 atm, cells do not grow and divide at pressures higher than 600 atm and cell death results at pressures higher than 1500 atm [34, 35]. While the effect of continuous pressure on the growth and cell morphology is explored to some extent, the effect of fluctuating pressure on the bacterial cells is relatively unknown.

E. coli growth rate decreases upon deviations in temperature and pressure from optimal growth pressure-temperature condition. Decrease in growth rate is proportional to the magnitude and duration of fluctuation of temperature and pressure. The growth rate of the bacterial cells is defined by the time at which the number of bacteria simply doubles. This population doubling time (T) is constant for a bacteria in same environmental conditions.

Inhibition of growth rate is one of the responses of bacteria at high pressures. At optimal growth condition *E. coli* have population doubling time (T) ≈ 30 minutes. The population doubling time increases on increasing pressure. Doubling time has sharp jump at pressure depending on the temperature. The growth rate of *E. coli* also inhibits at temperature different from 37°C . The decrease in growth rate depends upon the extent of deviating temperature from 37°C and pressure from an atmosphere [13].

Plasmid DNA

A plasmid is an extrachromosomal DNA capable of dividing inside the host cell. Plasmid DNA contains three main parts. (i) The origin of replication which initiates the replication. (ii) The selection site which makes bacterial cells capable of antibiotic resistance. (iii) The cloning site where the genes and marker are inserted according to use of the plasmid DNA [36]. We used a plasmid DNA having green fluorescent protein (GFP) fused with *mreB* gene [37].

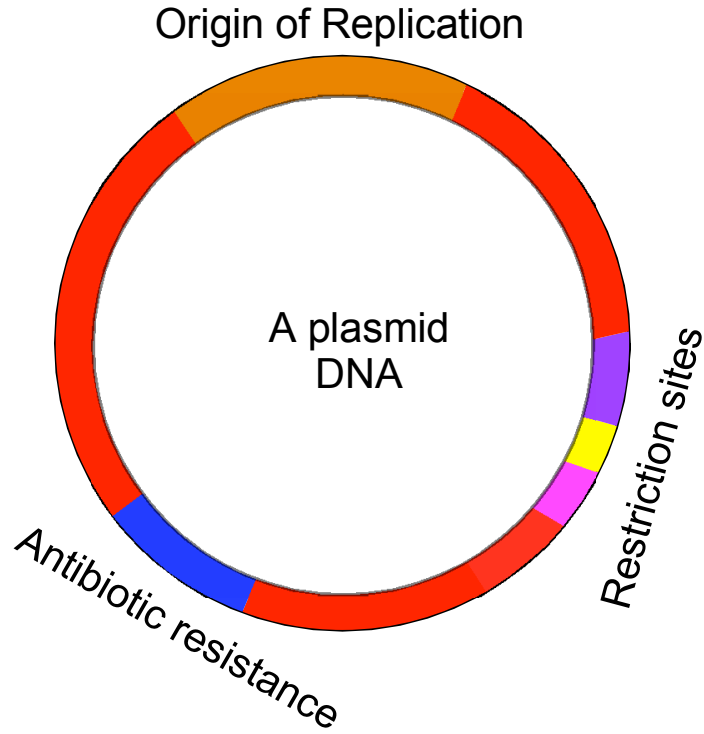


Figure 3: Schematic of a plasmid DNA.

Motivation

Bacterial cells encounter fluctuations in different physicochemical stresses and respond to such fluctuations. The response of the cells depends on the extent and type of the stresses applied. The response of bacterial cells to the fluctuating stress is relatively unknown. Here, we have studied the response of wild type *Escherichia coli* (*E. coli*) under fluctuating hydrostatic pressures ranging from 1 atm to 500 atm. High pressure acts as a stress to *E. coli* since these bacteria are adapted to grow optimally at atmospheric pressure. Cell division of *E. coli* is inhibited at high pressures resulting in increase in the length of the cells. It is also shown that the cell-length is reversible, in other words – bacterial cells revert back to normal size on a time scale that is proportional to the strength and time of continuous pressure applied upon relaxing the high pressure condition [Kumar, Libchaber, 2015]. Here we have explored the dynamics of reversibility of cellular phenotype with fluctuating pressure. Since

random fluctuations in pressure is hard to create in experiments, we have studied the cellular response in case of oscillatory pressures.

Research objective

The goal of these experiments is to establish the time-scale of cellular responses to a novel stress such as high hydrostatic pressure. Specifically, we have explored phenotypic variations occurring in *E. coli* at high pressures. Phenotypic studies include the morphological changes occurring in wild-type bacteria and wild-type bacteria cloned with a plasmid DNA at high continuous and oscillatory pressures.

Thesis outline

This thesis is divided into three chapters. Introduction of the problem is discussed with a brief description and development basis for further topics. This chapter mainly reviews the literature and establishes the framework for the research with definition of key points based on the previous works. We also describe briefly the studies related to this work carried out earlier.

Second chapter describes the experimental setup and molecular biology protocols used in the work.

Third chapter discusses the results. The response of wild-type bacteria and bacteria cloned with a plasmid DNA at high pressures is discussed thoroughly and how the morphology fluctuates in bacterial cells at high oscillating pressures. The morphological fluctuations of bacteria with plasmid are explained with and without the induction of gene expression.

The last chapter introduces a two population model of the bacterial cells based on the model developed in earlier research work to describe the experimental data. This chapter also summarizes the most important results of the research work.

Experimental Setup and Microbiology Protocols

Bacterial Strain

E. coli strain MC4100 was used for all the experiments performed in this work. MC4100 was cloned with a plasmid DNA containing mreB gene fused with green fluorescent protein (gfp). Two different variants namely –(i) wild-type MC4100 cells, (ii) MC4100 cloned with a plasmid DNA were used to probe the cellular response to high pressure. **Cell culture and media**

Bacteria are cultivated in Luria Broth (LB) [38]. which contains rich nutrients for the bacterial cells. The pH of the media is maintained at 7. Petri dishes containing ~ 25 mL are prepared adding 1.5% agar to the liquid medium. Carbenicillin of $50 \mu\text{g}$ per liter is added to grow the bacterial cells with a plasmid DNA. The bacterial stock is inoculated in solid media and incubated at 37°C for ~ 16 hours. A single colony from solid media is dissolved in 4 mL of liquid media. Then the bacterial sample is grown at 37°C on a shaker at 200 rpm until OD reaches to $0.4 - 0.6$. Then the sample is diluted to $\text{OD} \sim 0.05$ and loaded into the high pressure cell. Sample is kept at high pressure system at desired pressure and temperature of 37°C till growth reaches to the saturation regime.

High pressure setup

Schematic diagram for the growth of bacteria at high pressure is shown in Fig. 4. Bacterial sample in LB medium is loaded into a rectangular cuvette (vol: $400 \mu\text{L}$ Spectrocell, Oreland, PA,). The cuvette is closed with a teflon cap (E. I. DuPont de Nemours, Paris, France) . The cuvette is then loaded into the high pressure cell (ISS, Champaign, IL). Pressure is controlled by using a piston and is measured using a pressure gauge. Temperature is regulated using a circulating water bath (Neslab RTE7, Thermo Scientific, , Waltham, MA) containing water. Bacterial growth is obtained by measuring the intensity of the forward scattered light using a light detector(PDA 100A, Si amplified detector, Thorlabs inc, Newton, New Jersey, USA).The

intensity of the scattered light is converted into voltage and recorded with the aid of lab view (National Instruments, Austin, TX) software.

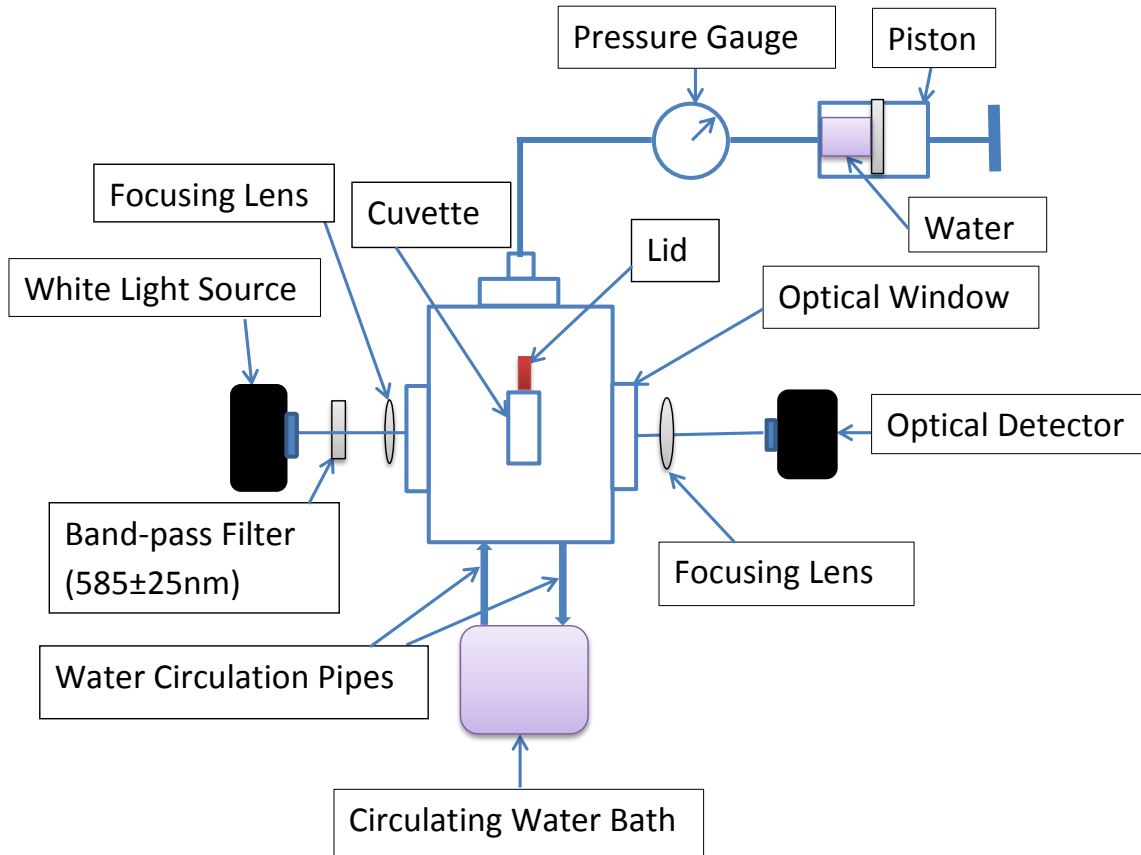


Figure 4: Schematic diagram of the experimental setup to grow bacteria at high pressures.

Imaging and analysis of the images

Bacterial sample is taken out at the end of the pressure experiment. We prepared the slides and images of the cells are acquired using a SPOT camera (Spot Imaging Solutions, MI) mounted on a Nikon EFD-3 microscope with 40X objective (both from Nikon corporation, Shinagawa, Tokyo, Japan). Images are acquired in ≈ 20 minutes to ensure there is no significant change in morphology. Images thus acquired are converted into binary images using imageJ. Cell length of each bacteria is extracted using MATLAB.

Phenotypic changes of Bacterial Cells with Continuous and Oscillatory Pressure

In this chapter, we describe the cellular changes in bacterial cells with continuous and oscillatory pressures in three different cases:

- Wild-type cells.
- Cells cloned with a plasmid DNA but no induction of gene expression.
- Cells cloned with a plasmid DNA and induction of gene expression.

Introduction of the additional DNA inside the cells leads to larger metabolic load on the cells because cells now have to replicate the additional DNA. Moreover, induction of gene expression introduces even larger metabolic load on the cells because cells will require energy (from metabolism) to carry out these additional functions. We find that, the presence or absence of these factors that require the cells to perform additional functions lead to different cellular responses to the stress (high hydrostatic pressure). Below, we summarize the results for the three cases explained above.

Response of wild-type cells (*E. coli* strain MC4100)

Comparison of morphology at normal and at high continuous pressures

Application of high hydrostatic pressure results in a decrease of growth rate. Moreover, high pressure is shown to inhibit cell division, resulting in an increase of the bacterial cell length. Furthermore, it was shown recently that, the lack of cell division at high pressures is stochastic in nature. While at atmospheric pressure, the probability that, a cell lacks a cell division is negligible the probability of lacking a cell division increases with pressure for DH5 α -strain of *E. coli*[13].

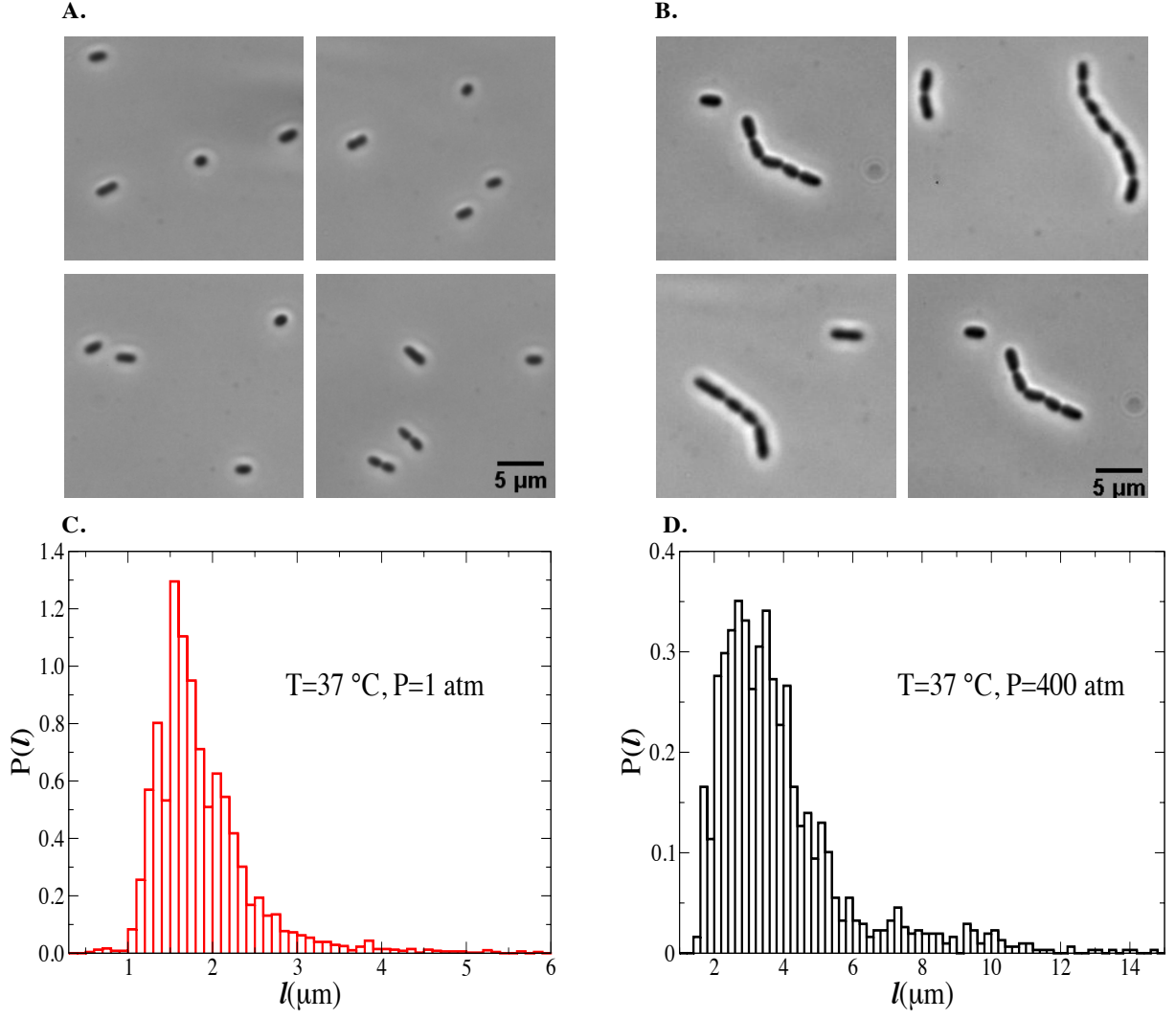


Figure 5: Bacterial cells at different continuous pressures. Representative images of the bacterial cells grown at $T=37^\circ\text{C}$ and continuous pressures of: (A) 1 atm, (B) 400 atm. $P(l)$ of bacterial cell lengths at $T=37^\circ\text{C}$ and pressures: (C), 1 atm, (D) 400 atm.

Figs. 5 (A) and (B), we show representative images of the bacterial cells at $P = 1$ atm and $P = 400$ atm. The data shows that, bacteria has high propensity of lacking cell division at high pressure condition as compared to bacterial cells at atmospheric pressure condition. The probability distribution, $P(\ell)$, of bacterial cell length, ℓ , for $P = 1$ atm and $P = 400$ atm are shown in Figs 5 (C) and (D) respectively. While $P(\ell)$ at $P = 1$ atm is narrow centered around the mean length, $\langle \ell \rangle \approx 2\mu\text{m}$ of bacterial cells, $P(\ell)$ at $P = 400$ atm is long-tailed centered around the mean length of $\approx 3\mu\text{m}$. Hence these results suggest that, the wild-type strain of *E. coli*, MC4100, studied here shows similar behavior of lack of cell division at high pressure however the probability of cell division to occur at high pressure is much larger as compared to DH5 α strain of *E. coli*. We next studied the response of bacterial cells to oscillating pressures. A schematic of the experiments is shown in Fig 6 (A). We apply a high pressure of 400 atm for 1 hour and let the system relax at atmospheric pressure over a time-scale τ . We performed these experiments for $P = 400$ atm where we observe a significant lack of cell division, and four different values of $\tau = 5$ min, 10 min, 15 min, and 20 min.

Comparison of morphology at different relaxation time (τ)

We studied the effect of oscillatory pressure to the morphology of the bacterial cells keeping at constant temperature (37°C). We oscillate the pressure for five different cycles. Then the images are taken as quickly as possible without being biased. The images thus obtained are quantified and individual length data are extracted. In figs 6 (B), (C), (D) and (E) we show the probability distribution, $P(\ell)$, of the length of bacterial cells for the values of $\tau = 5, 10, 15$ and 20 minutes respectively. We found that, the $P(\ell)$ is quite different compared to MC4100 wild-type. The tail of $P(\ell)$ is longest at $\tau=0$ minute as observed in wild-type MC4100. We further show that, the heterogeneity of the bacterial cell is much higher for bacteria cultivated at high pressure compared to bacteria cultivated at atmospheric pressure. Furthermore, the tail of the distribution decreases on increasing τ . Which is in agreement with the wild-type MC4100. The decrease in tail with increasing τ is much more faster

compared to wild-type MC4100. Moreover, the peak of the distribution shifts toward the smaller average length of the bacterial cells. These results imply that, the heterogeneity of the bacterial cells is smaller at higher τ 's. The $P(\ell)$ of the bacterial cells at $\tau = 20$ minutes is similar to the $P(\ell)$ of the bacterial cells grown at atmospheric pressure. $\langle \ell \rangle$ of the bacterial cell revert back to $\langle \ell \rangle$ at atmospheric pressure with τ . We observe that, when $\tau = 20$ minutes the heterogeneity and $\langle \ell \rangle$ revert back and comparable to the bacterial cells as grown at atmospheric pressure. The revert back of the cell length at oscillating pressure suggests that, the bacterial cells which are elongating due to application of the high pressure start to divide during the relaxation time. Relaxation of the pressure is more favorable condition for the bacterial cells to divide comparing to high continuous pressure. Bacterial cells respond to the relaxation and start to divide however the relaxation time is smaller compared to the time of high pressure applied. Bacterial cells show immediate response to the relaxation of the pressure. Application of τ to the bacterial cells grown at high pressure shows that, bacterial population with longer length decreases and revert back to bacteria with shorter length. This can be represented as bacteria with longer length phenotype switch to shorter length phenotype. The phenotypic switching is time dependent. We find the critical time of phenotypical switching is 20 minutes. Beyond this critical time, it does not incur any significant changes in $P(\ell)$ and $\langle \ell \rangle$ of the bacterial cells.

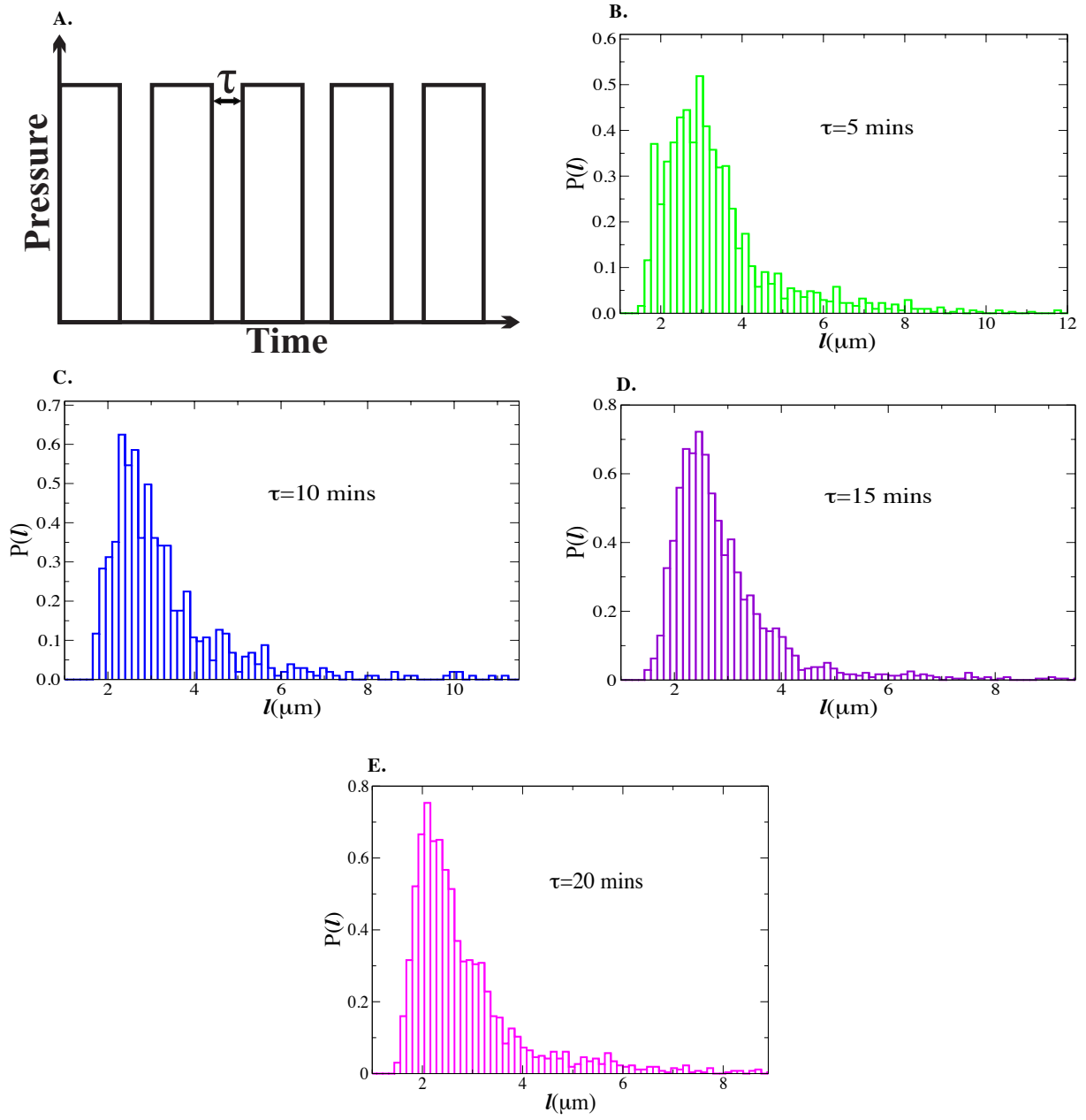


Figure 6: (A) Schematic diagram for the oscillatory pressure applied to the bacterial cells. $P(l)$ of bacterial cell length at $T = 37^\circ \text{C}$, $P = 400 \text{ atm}$ and relaxed for different scales of time: (B) 5 minutes, (C) 10 minutes, (D) 15 minutes and (E) 20 minutes.

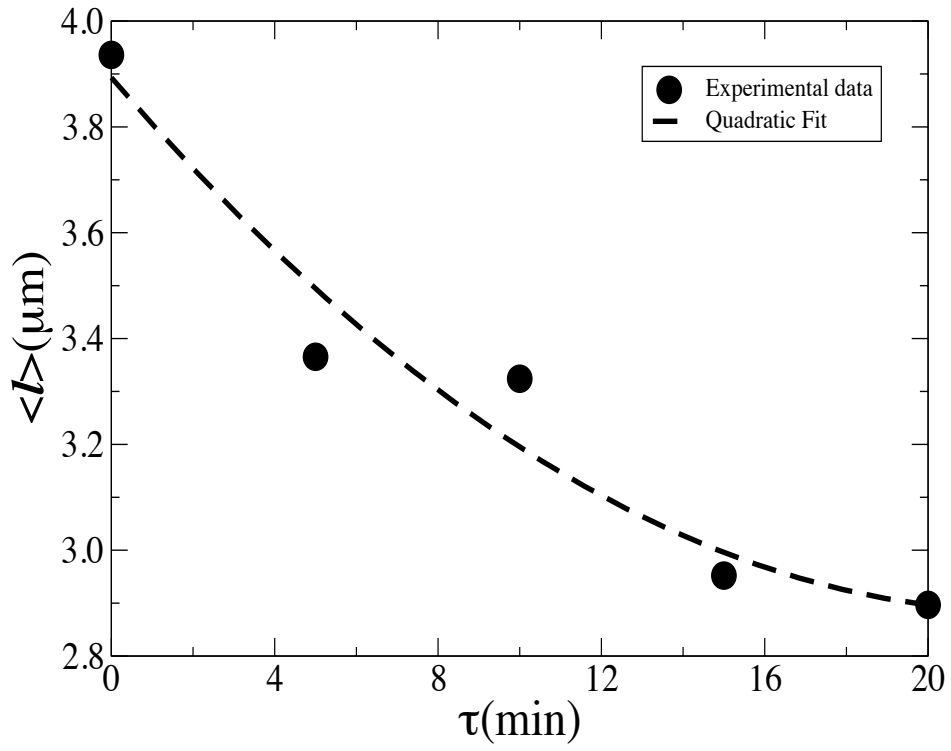


Figure 7: τ dependence of bacterial cells extracted from Fig 6. Black dots are experimental data-points and black solid line is second order polynomial fit to the experimental data-points.

Fig. 7 shows the τ dependence $\langle \ell \rangle$ of the bacterial cells. We fit the second order polynomial through experimentally observed $\langle \ell \rangle$. $\langle \ell \rangle$ decreases quadratically with τ . The length data are in agreement with $P(\ell)$ as described in Fig. 6. At $\tau = 20$ minutes $\langle \ell \rangle$ is found as $2.7\mu\text{m}$ which is close to the bacterial average length at atmospheric pressure= $2.5\mu\text{m}$. We next explored the response of the bacterial cells to the fast oscillation followed by growing the sample till saturation regime. We start the oscillatory pressure when bacterial cells are at saturation regime. First the bacterial cells are grown at high pressure of 450 atm for 5 hours. The pressure is continuously applied to 450 atm to bring the sample to saturation regime where is significant lack of cell division. Pressure of 450 atm is applied for an hour and released to 1 atm for different time scales. The application and relaxation of the pressure is applied for five different cycles. The duration of pressure applied and relaxed is made same with different time scales of $\tau = 5, 10, 15$, and 20 minutes.

Response of wild-type MC4100 to fast oscillations in pressure

Comparison of morphology at different relaxation time after growing to saturation regime(τ)

A schematic of the experiments is shown in Fig. 8 (A). Figs. 8 (B), (C), (D), (E) and (F) are $P(\ell)$ at $\tau = 5, 10, 15$, and 20 minutes respectively at constant temperature (37°C). We observe that, the tail of $P(\ell)$ and heterogeneity of probability distribution of bacterial cells decreases significantly when $\tau = 5$ minutes and again starts to increases till $\tau = 12$ minutes. There is no significant difference of $\langle \ell \rangle$ on further increasing τ . However, Fig. 8 shows that, the tail of the $P(\ell)$ of cell length decreases till $\tau = 5$ minutes and starts to increase further until the relaxation time reaches to 15 minutes. Beyond 15 minutes tail of $P(\ell)$ decreases. We further observe that, number of bacterial cells having length more than $8\mu\text{m}$ is very small for τ beyond 10 minutes. Hence, we conclude that, the sample is saturated beyond 12 minutes and there are no significant changes in $P(\ell)$ and $\langle \ell \rangle$. For the fast oscillatory pressure followed by the continuous pressure to bring the sample to saturation

regime, bacteria show two irregular phenotypic switching in their cell length.

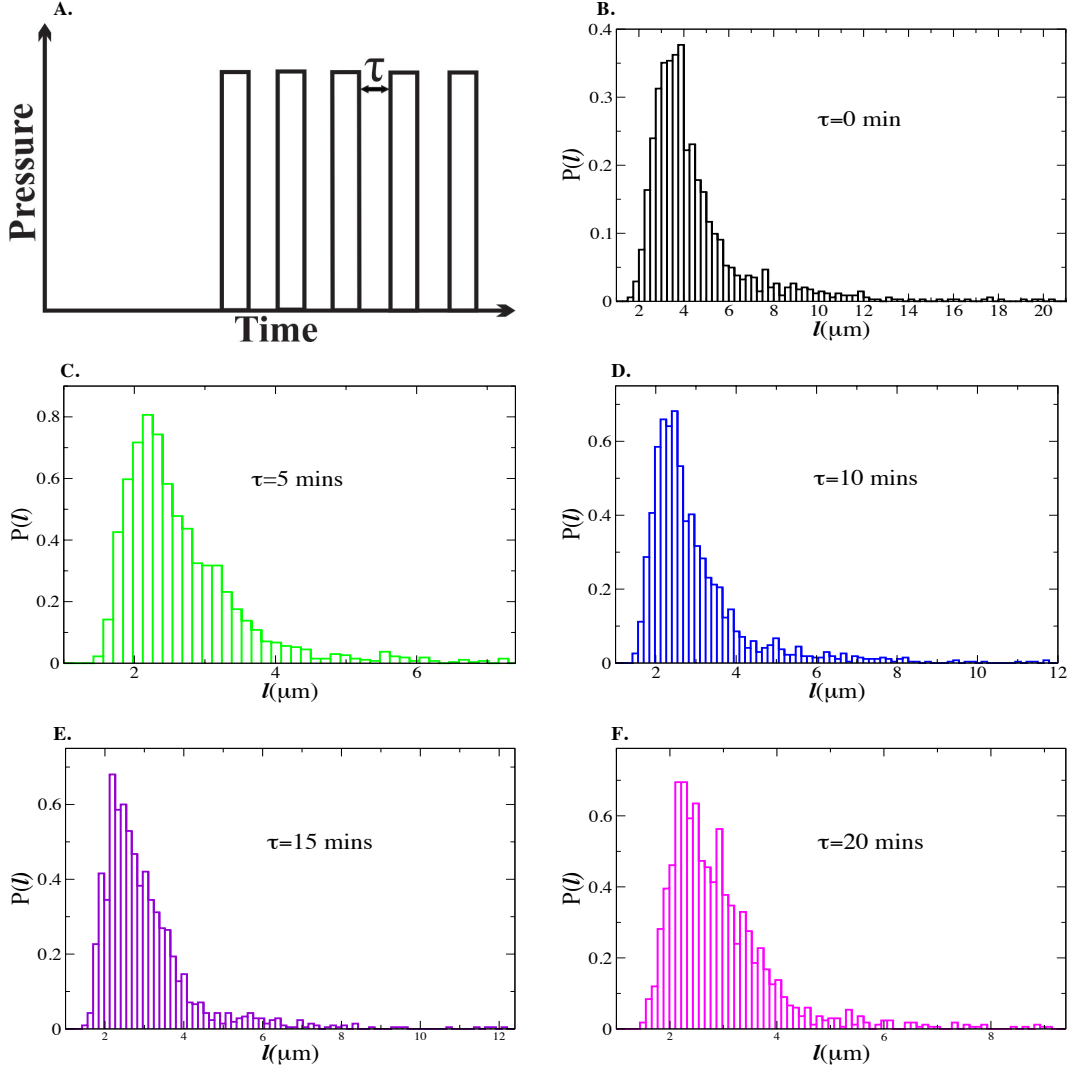


Figure 8: Bacterial cells are grown for five hours till they reach to the saturation regime at $T=37^\circ\text{C}$ and $P=450\text{ atm}$, then the time for applying pressure and relaxation is made same with varying scales. (A) Schematic diagram of application and relaxation of the pressures. $P(l)$ of bacterial cells at different scales of relaxation times: (B) $\tau=0$ minute, (C) $\tau=5$ minutes, (D) $\tau=10$ minutes, (E) $\tau=15$ minutes and (F) $\tau=20$ minutes.

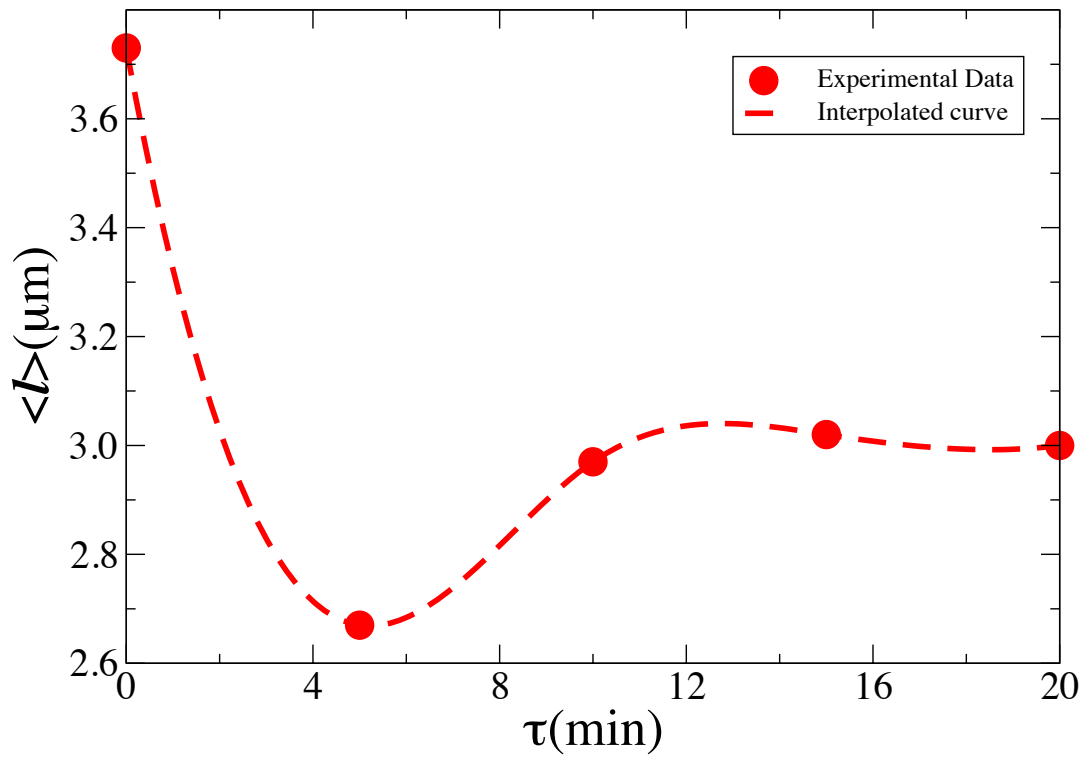


Figure 9: τ dependence average length of bacterial cells extracted from Fig 8. Red dots are experimental data-points and red dotted line is interpolated curve to the experimental data-points.

Fig. 9 shows the τ dependence $\langle \ell \rangle$ of the bacterial cells. We observe that, $\langle \ell \rangle$ is minimum when τ is 5 minutes. The minimum $\langle \ell \rangle$ is $2.7\mu\text{m}$ at $\tau = 5$ minutes, which is similar length as the minimum $\langle \ell \rangle$ of the bacterial cells at $\tau = 20$ minutes for the oscillatory pressure started from the beginning which we discussed in previous section. $\langle \ell \rangle$ increases when τ is increased on increasing τ up to 15 minutes. Beyond 15 minutes $\langle \ell \rangle$ decreases. When $\tau = 20$ minutes $\langle \ell \rangle$ is comparable to $\langle \ell \rangle$ when the sample grown in an oscillated pressure from the beginning.

Response of MC4100 cloned with a plasmid DNA

Comparison of morphology of at normal and at high continuous pressures

In Figs. 10 (A) and (B), we show representative images of the bacterial cells at $P = 1$ atm and at $P = 400$ atm. A comparison of Figs. 10 (B) and Figs. 5 (B) tells us that, the average length of the bacterial cells at 400 atm is significantly different between two samples—wild-type MC4100 and wild-type MC4100 cloned with a plasmid DNA. Furthermore, we find that, the lack of cell division of bacterial cells cloned with a plasmid DNA at 400 atmospheric pressure is much higher than the bacterial cells without a plasmid DNA. $P(\ell)$, of bacterial cell length, ℓ for $P = 1$ atm and $P = 400$ atm are shown in Figs 10 (C) and (D) respectively. While $P(\ell)$ at $P = 1$ atm is narrow centered around the mean length, $\langle \ell \rangle \approx 2.8\mu\text{m}$ of bacterial cells. $P(\ell)$ at $P = 400$ atm is long-tailed. $P(\ell)$ for the bacterial cells at atmospheric pressure is similar for both samples cloned with a plasmid DNA and without a plasmid DNA. The tail of the distribution at 400 atm is much higher compared to MC4100. Furthermore, the tail of the distribution is smooth in wild-type strain, the tail is multiple peaked in wild-type bacterial cells cloned with a plasmid DNA. Hence these results suggest that, the wild-type strain of E. coli, MC4100 cloned with a plasmid DNA shows similar behavior to the wild-type strain at atmospheric pressure but at 400 atm their behavior is significantly different.

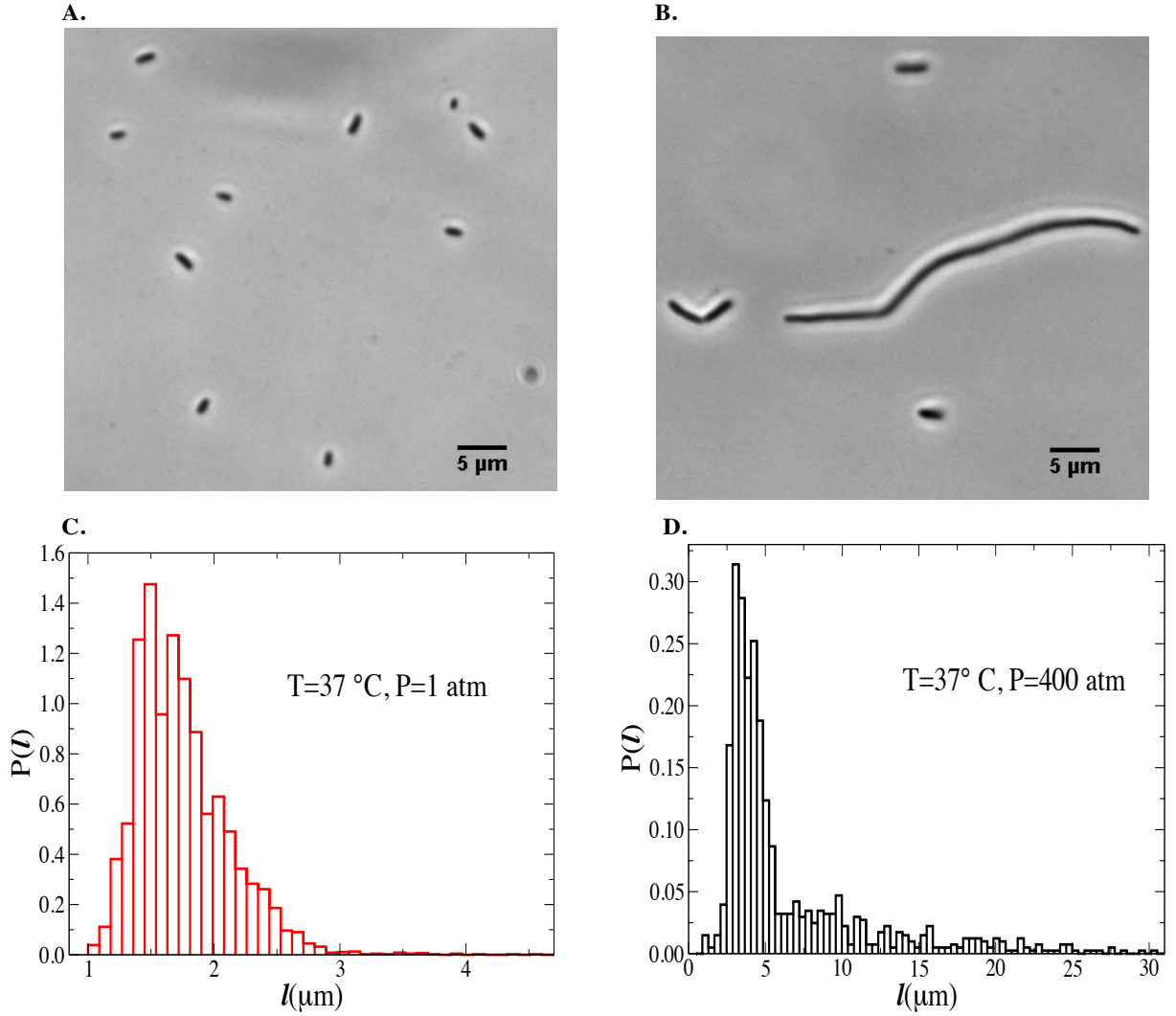


Figure 10: Bacterial cells cloned with a plasmid DNA at different continuous pressures. Representative images of the bacterial cells grown at $T=37^\circ\text{C}$ and continuous pressures of: (A) 1 atm, (B) 400 atm. $P(\ell)$ of bacterial cell lengths at $T=37^\circ\text{C}$ and pressures: (C) 1 atm, (D) 400 atm.

We next studied the response of bacterial cells to oscillating pressures. A schematic of the experiments is shown in Fig 11 (A). We apply a high pressure of 400 atm for 1 hour and let the system relax at atmospheric pressure over a time-scale τ . We performed these experiments for $P = 400$ atm, where we observe a significant lack of cell division and four different values of $\tau = 5$ min, 10 min, 15 min, and 20 min.

Comparison of morphology at different relaxation time (τ)

To investigate how the morphology of the wild-type bacterial cells cloned with a plasmid DNA deviates from wild-type MC4100, we oscillate the pressure keeping at constant temperature (37°C). At the end of 5 cycles of oscillating pressure, we analyzed the images taken after pressure and relaxation cycles and quantify the cell length data. In figs 6 (B), (C), (D) and (E) we show the probability distribution, $P(\ell)$ of the length of bacterial cells for the values of $\tau = 5, 10, 15$ and 20 minutes respectively. We found that, the tail of the distribution decreases on increasing the τ . Furthermore, the peak of the distribution shifts toward the smaller length of the bacterial cells. The results imply that, the heterogeneity of the bacterial cells is smaller at higher τ 's. The $P(\ell)$ of the bacterial cells at $\tau = 20$ minutes is comparable to the $P(\ell)$ of the bacterial cells grown at atmospheric pressure. $\langle \ell \rangle$ of the bacterial cell revert back to $\langle \ell \rangle$ at atmospheric pressure with τ . We observe that, when $\tau = 20$ minutes, the $\langle \ell \rangle$ as well as $P(\ell)$ are comparable to the bacterial sample harvested at atmospheric pressure. These results are similar to wild-type MC4100 described in previous section. The tail of the bacterial cell cloned with a plasmid DNA is longer than the wild-type bacterial cell. Both samples decrease their tail at higher values of τ 's. Interestingly, the tail of the bacterial cell with a plasmid DNA decreases much faster compared to wild-type cell and tails become comparable when $\tau = 20$ minutes to $P(\ell)$ of wild-type bacteria with no plasmid. The critical time for phenotypic switching is also found to be 20 minutes, exactly same as observed in wild-type cell.

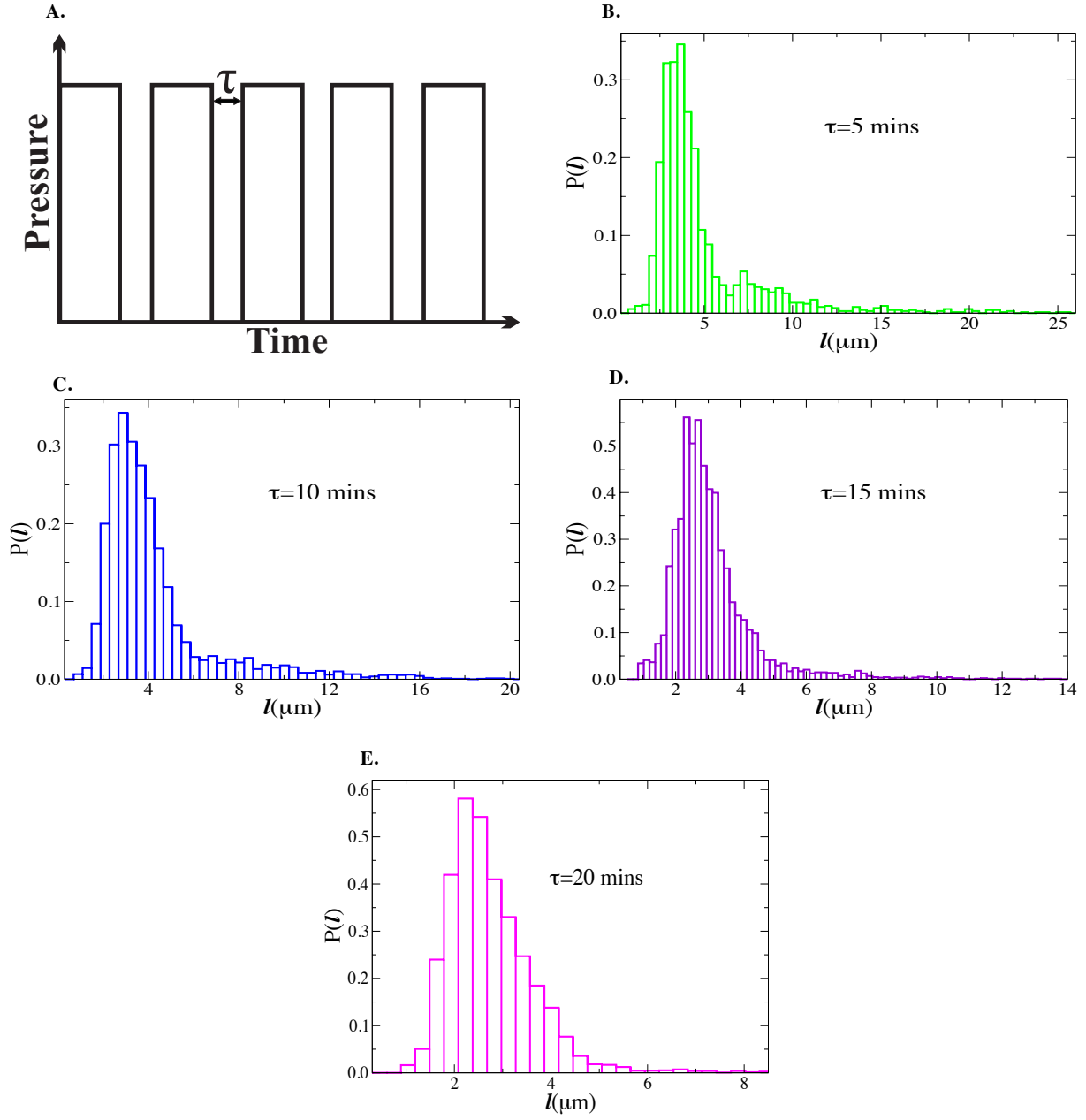


Figure 11: (A) Schematic diagram for the oscillatory pressure applied to the bacterial cells. $P(l)$ of bacterial cell length at $T=37^\circ\text{C}$, $P=400$ atm and relaxed for different scales of time: (B) 5 minutes, (C) 10 minutes, (D) 15 minutes and (E) 20 minutes.

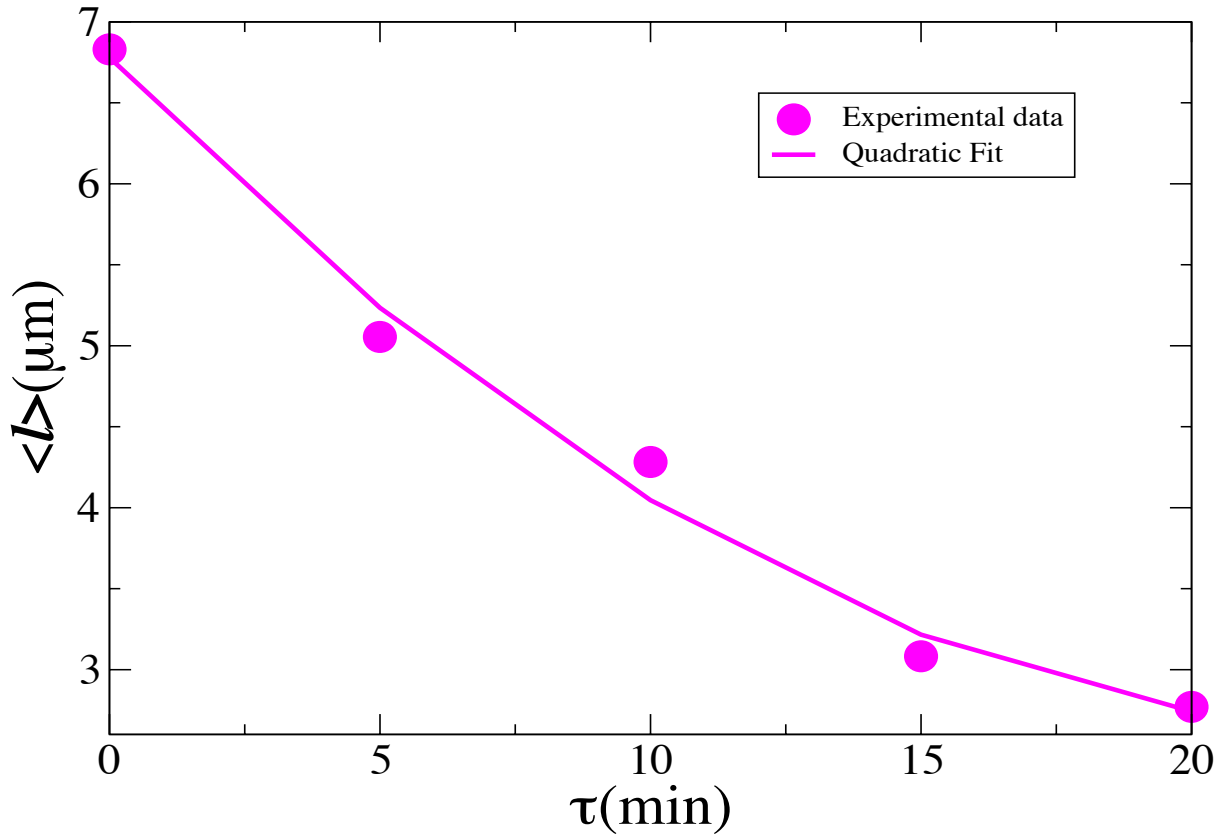


Figure 12: τ dependence average length of bacterial cells extracted from Fig 11. magenta dots are experimental data-points and magenta solid line is second order polynomial fit to the experimental data-points.

Fig. 12 shows τ dependence $\langle \ell \rangle$ of the bacterial cells cloned with a plasmid DNA. We fit a second-order polynomial through experimentally observed $\langle \ell \rangle$. $\langle \ell \rangle$ decreases quadratically with τ . The length data are in agreement with $P(\ell)$ as described in figs 11. At $\tau = 20$ minutes $\langle \ell \rangle$ is found to be $2.6\mu\text{m}$, which is close to the bacterial average length at atmospheric pressure and comparable to the length obtained for wild-type under similar conditions.

Comparison of $\langle \ell \rangle$ at different τ for different strains of bacterial cells

Fig. 13 shows the linear-log plot of phenotypic reversibility of different MC4100 samples under oscillatory pressure. Circles, squares and diamonds represent reversibility of wild-type MC4100, wild-type MC4100 cloned with a plasmid DNA without induction and MC4100 cloned with a a plasmid DNA and with induction respectively. Solid lines are corresponding guide to the eyes. Wild-type bacterial cells do not incur any additional metabolic stress, MC4100 cloned with a plasmid DNA have a moderate additional load as the plasmid DNAs are replicated as bacterial cells undergo cell division. Induction of gene expression in the cells with a plasmid DNA gives rise to a severe metabolic load arising due to replication of a plasmid DNA and production of the proteins. The production of proteins require energy which is supplemented to the cell by metabolic process. Which in turn, imposes higher stress to the bacterial cells at continuous high pressure. Wild-type MC4100 cells with no added metabolic load are stressed the least at high pressures. $\langle \ell \rangle$ of the bacterial cell is stress dependent. The most stressed bacterial strain exhibit the maximum average length ($35.42\mu\text{m}$) at continuous high pressure of 400 atm. The least stressed wild-type strain of bacterial cell has minimum average length. Interestingly, the cells revert back to the average cell length comparable to average cell length at atmospheric pressure over $\tau=20$ minutes. These results indicate that, bacterial cells exhibiting higher stress under the effect of continuous pressure also exhibit higher average length. The bacterial cells which are elongated longer revert back to the same average length with the cells that are elongated smaller due

to application of high pressure at the same scale of time. The reverting back to the same $\langle \ell \rangle$, irrespective of $\langle \ell \rangle$ at continuous pressure indicates that, bacterial cells show elastic property at oscillatory pressures.

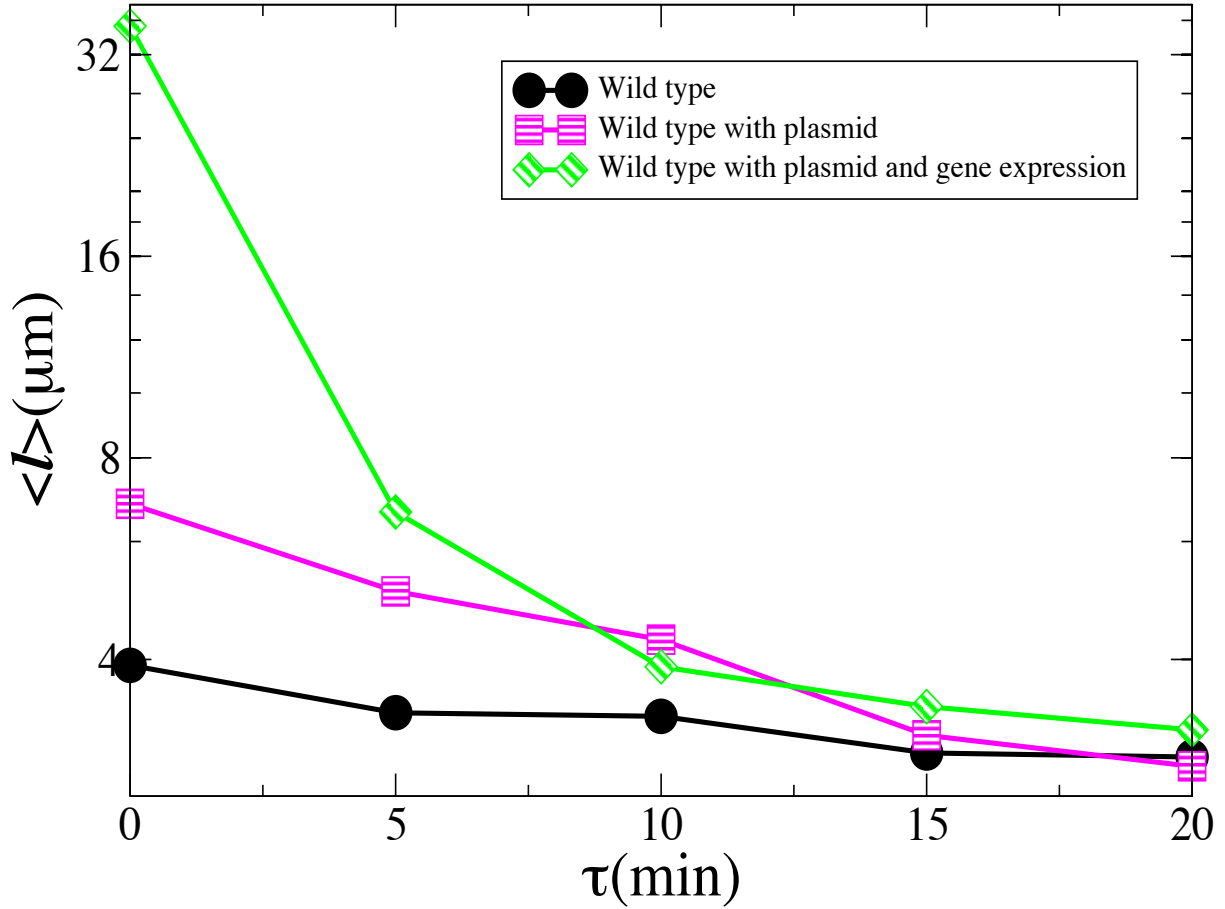


Figure 13: Phenotypic reversibility of bacterial cells at oscillatory pressures. Circles, squares and diamonds represent the reversibility of wild-type MC4100, wild-type MC4100 cloned with a plasmid DNA without induction and MC4100 cloned with a plasmid DNA and with induction. Solid lines are respective guides to the eye.

We next compared the morphology of wild-type MC4100 and MC4100 cloned with A plasmid DNA at continuous pressure of 400 atm. Fig. 14 (A) and (B) are the $P(\ell)$ of wild-type MC4100 and MC4100 cloned with a plasmid DNA.

Comparison of morphology of wild-type MC4100 and MC4100 cloned with a plasmid DNA at continuous high pressure

In Figs. 14 (A) and (B), we show the $P(\ell)$ of bacterial cells for wild-type MC4100 and MC4100 cloned with a plasmid DNA respectively. Both wild-type sample and a sample cloned with a plasmid DNA exhibit similar behavior at atmospheric pressure (fig. 5 (C) and fig. 10 (C)).

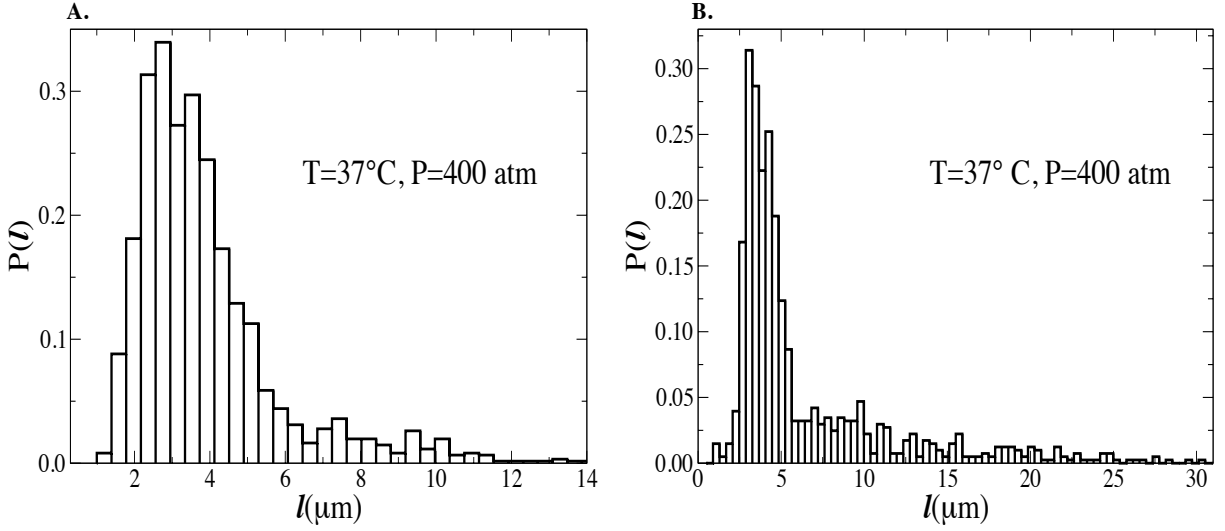


Figure 14: $P(\ell)$ at continuous pressure of 400 atm.(A), wild-type MC4100, (B),MC4100 cloned with a plasmid DNA.

However, the behavior of MC4100 cloned with a plasmid DNA is significantly different compared to wild-type MC4100 at high continuous pressure of 400 atm. $P(\ell)$ of wild-type cell is a long tailed Gaussian distribution with a single peak. We find that, $P(\ell)$ of MC4100 cloned with a plasmid DNA has longer tail compared to wild-type. Furthermore, the distribution exhibits multiple peaks. These results imply that, bacterial cells cloned with a plasmid DNA behave differently than the bacterial cells without a plasmid DNA. Moreover, the multiple peaks of $P(\ell)$ gradually decrease with τ . When τ is 20 minutes multiple peaked distribution turns to single peak long tailed distribution.

We next study the cause of the variability of cell length in wild-type MC4100 cloned with a

plasmid DNA. The stochastic cell division of two bacterial population is taken into account and $P(\ell)$ is described using an existing model. Fig. 15 and Fig. 16 describe the stochastic cell division of two populations and theoretical model to explain the morphological deviation of wild-type MC4100 cloned with a plasmid DNA from wild-type bacterial cell at continuous pressure of 400 atm respectively.

Theoretical model to explain cell-length variability

Fig. 14 shows the deviation of $P(\ell)$ of MC4100 cloned with a plasmid DNA from the wild-type MC4100. We describe the results by extending an existing model for a single population to two sub-population model. Our experimental results are described reasonably well by theoretical model.

Stochastic cell division of two populations

Fig. 15. shows the stochastic cell division of bacterial cell with two populations. The rectangles represent the bacterial cells. α_1 and α_2 represent the probability of dividing a bacterial cell dividing into two identical cells of two populations respectively. $\beta_1=(1-\alpha_1)$ and $\beta_2=(1-\alpha_2)$ are respective switching probabilities for the elongation of bacterial cells. Here, we assume that, the two populations behave differently and have different switching probabilities. Green rectangles represent bacterial cells dividing normally with probability α and purple rectangles represent bacterial cells switching to elongated cells with probability β . During the application of high pressure, once a cell does not divide in a given generation, it does not divide in any of the following generations. Cell morphology is irreversible process during the application of the continuous high pressure. [13].

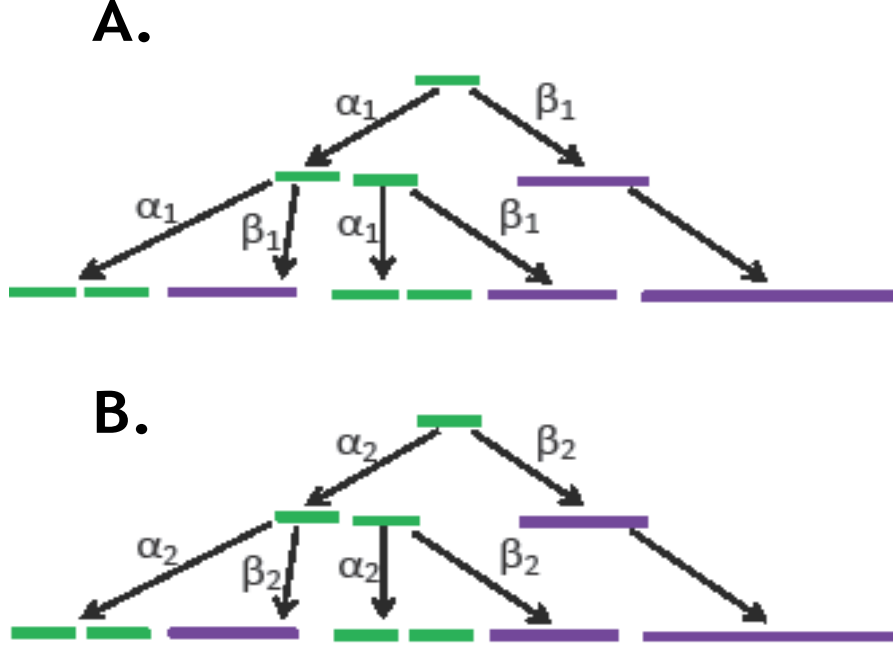


Figure 15: Schematic of stochastic cell division of two populations.

Theoretical model with two sub-populations

We further look at the existing model developed for bacterial cell division at continuous high pressure. We applied the model with an assumption of two sub-populations. We calculated the variance (σ_0) and average length (ℓ_0) of the bacterial sample grown at atmospheric pressure. The probability distribution at the end of n generation of a single population model reads as,

$$P_n(\ell) = \sum_{a=0}^n \left(\left(\frac{\beta}{2(1-\beta)} \right)^a \frac{1 - \frac{3}{2}\beta}{(1-\beta)[1 - (\frac{\beta}{2(1-\beta)})^{n+1}]} \frac{1}{\sqrt{2\pi\sigma_0^2 2^{2a}}} e^{-\frac{(1-2^a\ell_0)^2}{2 \cdot 2^{2a}\sigma_0^2}} \right) \quad (1)$$

Where, β is the switching probability of bacterial cells, n is number of generations, ℓ_0 and σ_0 are the average length and standard deviation of $P(\ell)$ of the bacterial cells cultivated at atmospheric pressure [13]. We further extended the model to two sub-populations. The probability distribution at the end of n generation of the bacterial growth at high continuous

pressure can be written as,

$$P_n(\ell) = \sum_{a=0}^n \left(\left(\frac{\beta_1}{2(1-\beta_1)} \right)^a \frac{1 - \frac{3}{2}\beta_1}{(1-\beta_1)[1 - (\frac{\beta_1}{2(1-\beta_1)})^{n+1}]} \frac{1}{\sqrt{2\pi\sigma_0^2 2^{2a}}} e^{-\frac{(1-2^a\ell_0)^2}{2 \cdot 2^{2a}\sigma_0^2}} + \left(\frac{\beta_2}{2(1-\beta_2)} \right)^a \frac{1 - \frac{3}{2}\beta_2}{(1-\beta_2)[1 - (\frac{\beta_2}{2(1-\beta_2)})^{n+1}]} \frac{1}{\sqrt{2\pi\sigma_0^2 2^{2a}}} e^{-\frac{(1-2^a\ell_0)^2}{2 \cdot 2^{2a}\sigma_0^2}} \right) \quad (2)$$

We next fit Eq. (2) with our experimental data for MC4100 cloned with a plasmid DNA. The multiple peaked distribution suggests that, there are two sub-populations dividing with different switching probabilities. f_1 and f_2 are the fractions of two populations respectively. In Fig. 16, blue histogram is experimental data and magenta curve is the model fit through the histogram. From fitting, we found that, $\beta_1=0.1$, $\beta_2=0.5$, $f_1=0.58$, $f_2=0.42$ and $n=5$. The theoretical curve fits well with experimental histogram. This fitting shows that, the deviation of morphology of MC4100 cloned with a plasmid DNA from the wild-type MC4100 is due to two sub-populations of bacterial cells at high continuous pressure arising from different switching probabilities.

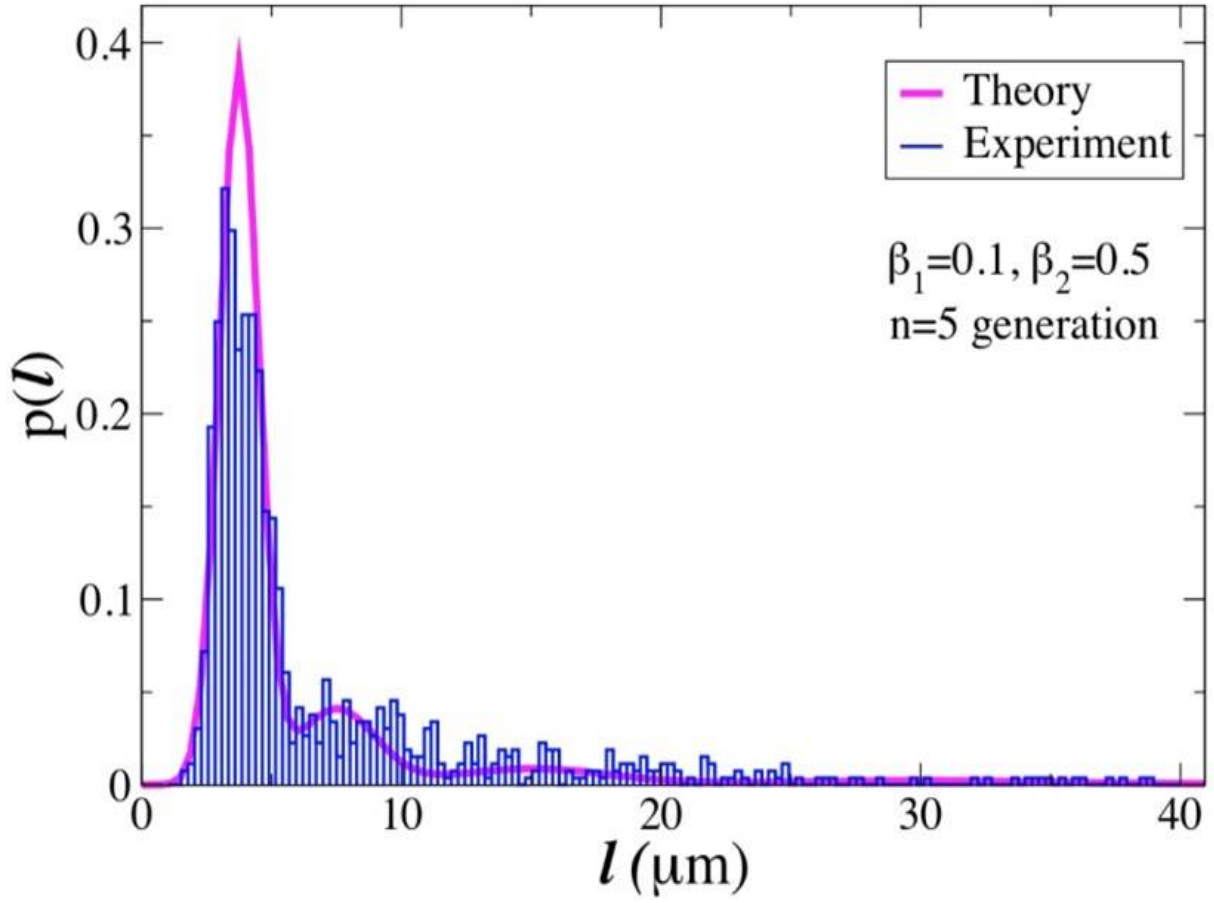


Figure 16: Theoretical model from equation (2), fitting to the experimental data, obtained for MC4100 with a plasmid DNA at high continuous pressure. Blue histogram is the experimental data, magenta curve is the theoretical curve with two switching probabilities 0.1 and 0.5 for five generations.

Discussion

The $\langle \ell \rangle$ of the rod shaped bacterial cells is proportional to the extent and duration of hydrostatic pressure applied. At high pressures of 500 atm, the bacterial cells not only elongate but also divide resulting into larger heterogeneity of bacterial population. The elongation and division of the bacterial cells depend on the continuous pressure applied. Continuous hydrostatic pressure causes bacterial cells to increase in length if the cells do not divide at a given generation. Our results show similar elongation behavior of the cell as observed for DH5 α strain, however the switching probability(β) is smaller [13]. β varies from strain to strain of the bacterial cells even though they have same genome. The addition of extracellular plasmid DNA results in a higher stress and larger propensity of lack of cell division during the application of continuous high pressure. Average bacterial length is τ dependent under the effect of an oscillating pressure. For the bacterial strain studied here and the oscillation starting from the beginning of the application of high pressure, the critical time for bacterial cells to revert back is found as $\tau \approx 20$ minutes. The behavior of the bacterial cells at oscillating pressure applied after the sample is grown to the saturation regime at continuous pressure is different from the same sample under the application of an oscillatory pressure from the beginning. Bacterial cells has minimum $\langle \ell \rangle$ and small heterogeneity at $\tau = 5$ minutes. Both the $\langle \ell \rangle$ and heterogeneity increase further until τ reaches 12 minutes. The $P(\ell)$ and $\langle \ell \rangle$ saturate on further increasing τ . Bacterial morphology reverts back in time when the continuous pressure applied on the sample is removed [Kumar, Libchaber, 2015] implies that, Pressure relaxation or release is more favorable for bacterial cell division. Hence, the $\langle \ell \rangle$ and heterogeneity decrease with an oscillatory pressure and depend on τ . Bacterial cells that, are elongated during the application of continuous high pressure divide during the relaxation of pressure. The time scale of the relaxation of pressure and bacterial cell division time are important to determine the fraction of sub-populations dividing while the pressure is relaxed. The population doubling time of E. coli in laboratory condition is ≈ 20 minutes. After the relaxation time scale of ≈ 20 minutes, cells divide more or less

completely. Both $P(\ell)$ and $\langle \ell \rangle$ of bacterial cell for $\tau = 20$ minutes are comparable. The process of cell division and the role of the genes and their interaction are related to the process of phenotypic dynamic reversibility studied here. We have studied the response at cellular level. To understand the effect of cell at genomic level, it needs further experiments. These results are helpful in understanding the response of cells to the fluctuations in environments and hence a better understanding reason of sustaining and vanishing of the organisms from nature.

Conclusion

We have studied the response of bacterial cells in fluctuating pressures. Bacteria tend to lack cell division at high pressure resulting in an increase of their average length at continuous high pressure. The application of the oscillatory pressure cause the elongated bacterial cells to divide ensuring a decrease in average length of the bacterial sample. The wild-type MC4100 cells cloned with a plasmid DNA without induction of gene expression are stressed and hence elongate more as compared to the wild-type MC4100. When the gene expression is induced, the stress as well as elongation is much higher. Response of bacterial cells cloned with a plasmid DNA is similar to the response shown by wild-type cells at atmospheric pressure. However, the response is significantly different at high pressure. We find two differences at pressure of 400 atm. (i) the average length is longer for the bacterial cells cloned with a plasmid DNA. (ii) the probability distribution of the bacterial cells cloned with a plasmid DNA show multiple peaks but the wild-type cells show a single peak. The multiple peaked distribution gradually changes to a single peaked distribution on increasing the relaxation time. The distribution is single peaked when the relaxation time is 20 minutes. The bacterial sample sample cloned with a plasmid DNA acts as two sub-populations with different switching probabilities at continuous high pressure. Two different switching probabilities govern multiple peak seen in the probability distribution of cells at high continuous pressure.

Relaxation time of the oscillatory pressure plays an important role in the average length of the bacterial cells. The average length of the bacterial population reverts to the length close to average length of bacterial sample cultivated at an atmospheric pressure when the relaxation time is ≈ 20 minutes. All the samples we studied here has average length $\approx 2.8\mu\text{m}$ irrespective of the average length at continuous high pressures.

Bibliography

- [1] A Aristides Yayanos, Allan S Dietz, and R Van Boxtel. Obligately barophilic bacterium from the mariana trench. *Proceedings of the National Academy of Sciences*, 78(8):5212–5215, 1981.
- [2] Chiaki Kato, Lina Li, Yuichi Nogi, Yuka Nakamura, Jin Tamaoka, and Koki Horikoshi. Extremely barophilic bacteria isolated from the mariana trench, challenger deep, at a depth of 11,000 meters. *Applied and environmental microbiology*, 64(4):1510–1513, 1998.
- [3] Karsten Pedersen. Microbial life in deep granitic rock. *FEMS Microbiology Reviews*, 20(3-4):399–414, 1997.
- [4] Claude E Zobell and Richard Y Morita. Barophilic bacteria in some deep sea sediments. *Journal of Bacteriology*, 73(4):563, 1957.
- [5] Christa Schleper, G Pühler, B Kühlmorgen, and Wolfram Zillig. Life at extremely low ph. *Nature*, 375(6534):741–742, 1995.
- [6] Kōki Horikoshi and Teruhiko Akiba. *Alkalophilic microorganisms: a new microbial world*. Springer Verlag, 1982.
- [7] WD Grant. Life at low water activity. *Philosophical Transactions of the Royal Society B: Biological Sciences*, 359(1448):1249–1267, 2004.
- [8] Roger Sassen, Ian R MacDonald, Norman L Guinasso, Samantha Joye, Adolfo G Requejo, Stephen T Sweet, Javier Alcalá-Herrera, Debra A DeFreitas, and David R Schink. Bacterial methane oxidation in sea-floor gas hydrate: significance to life in extreme environments. *Geology*, 26(9):851–854, 1998.
- [9] Rocco L. Mancinelli Rothschild, Lynn J. Life in extreme environments. *Nature*, 409(6823):1092–1101, 2001.
- [10] DA Ratkowsky, June Olley, TA McMeekin, and A Ball. Relationship between temperature and growth rate of bacterial cultures. *Journal of Bacteriology*, 149(1):1–5, 1982.
- [11] Stephen Cooper. Bacterial growth and division. *Encyclopedia of Molecular Cell Biology and Molecular Medicine*, 2006.
- [12] Richard W Young. Cell differentiation in the retina of the mouse. *The Anatomical Record*, 212(2):199–205, 1985.
- [13] Pradeep Kumar and Albert Libchaber. Pressure and temperature dependence of growth and morphology of escherichia coli: experiments and stochastic model. *Biophysical journal*, 105(3):783–793, 2013.
- [14] Dann Huh and Johan Paulsson. Non-genetic heterogeneity from stochastic partitioning at cell division. *Nature genetics*, 43(2):95–100, 2011.

- [15] Nikos V Mantzaris. From single-cell genetic architecture to cell population dynamics: quantitatively decomposing the effects of different population heterogeneity sources for a genetic network with positive feedback architecture. *Biophysical journal*, 92(12):4271–4288, 2007.
- [16] Jacob Hanna, Krishanu Saha, Bernardo Pando, Jeroen Van Zon, Christopher J Lengner, Menno P Creyghton, Alexander van Oudenaarden, and Rudolf Jaenisch. Direct cell reprogramming is a stochastic process amenable to acceleration. *Nature*, 462(7273):595–601, 2009.
- [17] Richard Losick and Claude Desplan. Stochasticity and cell fate. *science*, 320(5872):65–68, 2008.
- [18] Purnananda Guptasarma. Does replication-induced transcription regulate synthesis of the myriad low copy number proteins of escherichia coli. *Bioessays*, 17(11):987–997, 1995.
- [19] Kurt Nordstrom and Stuart J Austin. Mechanisms that contribute to the stable segregation of plasmids. *Annual review of genetics*, 23(1):37–69, 1989.
- [20] C William Birky Jr. The partitioning of cytoplasmic organelles at cell division. *International review of cytology. Supplement*, 15:49–89, 1982.
- [21] Joe Lutkenhaus and and SG Addinall. Bacterial cell division and the z ring. *Annual review of biochemistry*, 66(1):93–116, 1997.
- [22] Xiaolan Ma, David W Ehrhardt, and William Margolin. Colocalization of cell division proteins ftsz and ftsa to cytoskeletal structures in living escherichia coli cells by using green fluorescent protein. *Proceedings of the National Academy of Sciences*, 93(23):12998–13003, 1996.
- [23] Xunde Wang, JIAN Huang, Amit Mukherjee, Chune Cao, and Joe Lutkenhaus. Analysis of the interaction of ftsz with itself, gtp, and ftsa. *Journal of bacteriology*, 179(17):5551–5559, 1997.
- [24] Joseph C Chen, David S Weiss, Jean-Marc Ghigo, and Jon Beckwith. Septal localization of ftsq, an essential cell division protein in escherichia coli. *Journal of bacteriology*, 181(2):521–530, 1999.
- [25] David S Weiss, Joseph C Chen, Jean-Marc Ghigo, Dana Boyd, and Jon Beckwith. Localization of ftsi (pbp3) to the septal ring requires its membrane anchor, the z ring, ftsa, ftsq, and ftsl. *Journal of bacteriology*, 181(2):508–520, 1999.
- [26] Xiaolan Ma and William Margolin. Genetic and functional analyses of the conserved c-terminal core domain of escherichia coli ftsz. *Journal of bacteriology*, 181(24):7531–7544, 1999.

- [27] Neena Din, Ellen M Quardokus, Marcella J Sackett, and Yves V Brun. Dominant c-terminal deletions of ftsz that affect its ability to localize in caulobacter and its interaction with ftsa. *Molecular microbiology*, 27(5):1051–1063, 1998.
- [28] Xuan-Chuan Yu and William Margolin. Ca²⁺-mediated gtp-dependent dynamic assembly of bacterial cell division protein ftsz into asters and polymer networks in vitro. *The EMBO journal*, 16(17):5455–5463, 1997.
- [29] Danièle Joseleau-Petit, Daniel Vinella, and Richard D’Ari. Metabolic alarms and cell division in escherichia coli. *Journal of bacteriology*, 181(1):9–14, 1999.
- [30] Amit Mukherjee and Joe Lutkenhaus. Dynamic assembly of ftsz regulated by gtp hydrolysis. *The EMBO journal*, 17(2):462–469, 1998.
- [31] Masaki Osawa, David E Anderson, and Harold P Erickson. Reconstitution of contractile ftsz rings in liposomes. *Science*, 320(5877):792–794, 2008.
- [32] Akihiro Ishii, Takako Sato, Masaaki Wachi, Kazuo Nagai, and Chiaki Kato. Effects of high hydrostatic pressure on bacterial cytoskeleton ftsz polymers in vivo and in vitro. *Microbiology*, 150(6):1965–1972, 2004.
- [33] Claude E Zobell and Andre B Cobet. Growth, reproduction, and death rates of escherichia coli at increased hydrostatic pressures. *Journal of bacteriology*, 84(6):1228–1236, 1962.
- [34] Timothy J. Welch, Anne Farewell, Frederick C Neidhardt, and Douglas H Bartlett. Stress response of escherichia coli to elevated hydrostatic pressure. *Journal of Bacteriology*, 175(22):7170–7177, 1993.
- [35] Yu-Ling Shih and Lawrence Rothfield. The bacterial cytoskeleton. *Microbiology and Molecular Biology Reviews*, 70(3):729–754, 2006.
- [36] Gloria del Solar, Rafael Giraldo, María Jesús Ruiz-Echevarría, Manuel Espinosa, and Ramón Díaz-Orejas. Replication and control of circular bacterial plasmids. *Microbiology and molecular biology reviews*, 62(2):434–464, 1998.
- [37] Joseph Sambrook, Edward F Fritsch, Tom Maniatis, et al. *Molecular cloning*, volume 2. Cold spring harbor laboratory press New York, 1989.
- [38] G Bertani. Studies on lysogenesis i.: The mode of phage liberation by lysogenic escherichia coli1. *Journal of bacteriology*, 62(3):293, 1951.

Appendix

Below, we list the MATLAB code, which was used to quantify the binary images to obtain the cell length data. We selected the lower cut-off and upper cut-off lengths to be 0.5 and 40 μm respectively. We used the pixel of each image and fit a polynomial through the curvature of the bacterial cells in both x-axis and y-axis. We further take into account of the largest curvature among both axes. Finally, the length of the curvature is extracted. The length of the curvature provides us the length data. The length data are analyzed to get the probability distribution and the average length for respective experiments.

```
clear all
%choose a cutoff length for the bacteria
cutoffL2=40;
cutoffL1=0.5;
scale100x=8;
%Number of real bacteria detected for each image files
nBacFound=1;
%Loop for images
for nimage=1:129
    nimage
    imfile = sprintf('Image%d.tif', nimage);
    BW=imread(imfile);
    BW=1-BW;
    [B,L,N,A] = bwboundaries(BW, 'noholes');

    arcL = zeros(1,N);
    for i=1:N
        d=cell2mat(B(i));
        minY = min(d(:,1));
        maxY = max(d(:,1));
        maxX = max(d(:,2));
        minX = min(d(:,2));
        dX = maxX-minX;
        dY = maxY-minY;

        if(dX>=dY & dX>2)
            lengthX = maxX-minX+1;
            meanYvals = zeros(lengthX,1);
            n=1;
            for k=minX:maxX
                idx = find(d(:,2)==k);
                yVals = d(idx);
                diam(n) = length(min(yVals):max(yVals));
                meanYvals(n) = sum(min(yVals):max(yVals))/(length(min(yVals):max(yVals)));
                % take the average y-values for a given x
                n=n+1;
            end
            % now we have y as a function of x for each connected component of the
            % image.
            X = minX:maxX;
            X=X';
            Y = meanYvals;
```



```

    %determine the order of polynomial
nOrder = floor(dX/200)+2;
parFit = polyfit(X,Y,nOrder);
derL=0;
func = 0;
for np=1:nOrder
    derL = derL+(nOrder-np+1)*parFit(np)*X.^(nOrder-np);
end

for np=1:nOrder+1
    func = func + parFit(np)*X.^(nOrder-np+1);
end

arcL(i) = sum(sqrt(1+derL.*derL));
arcL(i) = arcL(i)/scale100x;
meanDiam(i) = mean(diam)/scale100x;
end

if(dY>dX & dY>2)
    lengthX = maxY-minY+1;
    meanYvals = zeros(lengthX,1);
    n=1;
    for k=minY:maxY
        idx = find(d(:,1)==k);
        yVals = d(idx,2);
        meanYvals(n) = sum(min(yVals):max(yVals))/(length(min(yVals):max(yVals)));
        % take the average y-values for a given x
        diam(n) = length(min(yVals):max(yVals));
        n=n+1;
    end
    % now we have y as a function of x for each connected component of the
    % image.

X = minY:maxY;
X=X';
Y = meanYvals;
%determine the order of polynomial
nOrder = floor(dY/200)+2;
parFit = polyfit(X,Y,nOrder);
derL=0;
func = 0;
for np=1:nOrder
    derL = derL+(nOrder-np+1)*parFit(np)*X.^(nOrder-np);
end

for np=1:nOrder+1
    func = func + parFit(np)*X.^(nOrder-np+1);
end

arcL(i) = sum(sqrt(1+derL.*derL));
arcL(i) = arcL(i)/scale100x;
meanDiam(i) = mean(diam)/scale100x;
end

```

```

end

% arcL contains the length of all the bacteria. Now choose only the
% bacteria which are properly oriented. For that we will choose a cutoff
% length (unless otherwise one is looking at a different bacteria).
n=1;
for k=1:length(arcL)
    if(arcL(k)>cutoffL2)
        imfile
        break;
    end
    if(arcL(k)>cutoffL1 && arcL(k)<cutoffL2)
        realL(n)=arcL(k);
        bacLength(nBacFound)=realL(n);
        nBacFound = nBacFound+1;
        n=n+1;
    end
end
end
% fill the array of lengths with the length found for each image files

%fill the connected components with different color
imshow(label2rgb(L, @jet, [.5 .5 .5]))
hold on
%outline the boundaries only for the bacteria larger than cutoffL

% for k = 1:length(arcL)
%     if(arcL(k)>cutoffL1)
%         boundary = B{k};
%         plot(boundary(:,2), boundary(:,1), 'w', 'LineWidth', 2)
%     end
% end

```